

This article was downloaded by: [University of Haifa Library]

On: 08 August 2012, At: 14:21

Publisher: Taylor & Francis

Informa Ltd Registered in England and Wales Registered Number: 1072954 Registered office: Mortimer House, 37-41 Mortimer Street, London W1T 3JH, UK



## Molecular Crystals and Liquid Crystals

Publication details, including instructions for authors and subscription information:

<http://www.tandfonline.com/loi/gmcl20>

### Cationic Iridium Complexes with Phenylpyridine and Strong Ancillary Ligands

Ho Wan Ham<sup>a</sup> & Young Sik Kim<sup>a b</sup>

<sup>a</sup> Department of Information Display, Hongik University, Seoul, Korea

<sup>b</sup> Department of Science, Hongik University, Seoul, Korea

Version of record first published: 19 Apr 2010

To cite this article: Ho Wan Ham & Young Sik Kim (2010): Cationic Iridium Complexes with Phenylpyridine and Strong Ancillary Ligands, *Molecular Crystals and Liquid Crystals*, 520:1, 108/[384]-115/[391]

To link to this article: <http://dx.doi.org/10.1080/15421400903582865>

PLEASE SCROLL DOWN FOR ARTICLE

Full terms and conditions of use: <http://www.tandfonline.com/page/terms-and-conditions>

This article may be used for research, teaching, and private study purposes. Any substantial or systematic reproduction, redistribution, reselling, loan, sub-licensing, systematic supply, or distribution in any form to anyone is expressly forbidden.

The publisher does not give any warranty express or implied or make any representation that the contents will be complete or accurate or up to date. The accuracy of any instructions, formulae, and drug doses should be independently verified with primary sources. The publisher shall not be liable for any loss, actions, claims, proceedings, demand, or costs or damages whatsoever or howsoever caused arising directly or indirectly in connection with or arising out of the use of this material.

# Cationic Iridium Complexes with Phenylpyridine and Strong Ancillary Ligands

HO WAN HAM<sup>1</sup> AND YOUNG SIK KIM<sup>1,2</sup>

<sup>1</sup>Department of Information Display, Hongik University, Seoul, Korea

<sup>2</sup>Department of Science, Hongik University, Seoul, Korea

*We report the theoretical studies of cationic Ir(III) complexes with phenylpyridine and phosphines, [trans-Ir(dfMeppy)<sub>2</sub>(PPh<sub>2</sub>Me)<sub>2</sub>]<sup>+</sup> and [cis-Ir(dfMeppy)<sub>2</sub>(PPh<sub>2</sub>Me)<sub>2</sub>]<sup>+</sup>. To gain insight into the factors responsible for the emission color change and the different quantum yields, we perform DFT and TDDFT calculations on the ground and excited states of these complexes, including solvation effects on the calculation of the excited states. [Trans-Ir(dfMeppy)<sub>2</sub>(PPh<sub>2</sub>Me)<sub>2</sub>]<sup>+</sup> produces the PL emission at 450 and 475 nm, whereas [cis-Ir(dfMeppy)<sub>2</sub>(PPh<sub>2</sub>Me)<sub>2</sub>]<sup>+</sup> produces the PL emission at 442 and 470 nm, respectively. The computational study allows us to reveal that the position of the PPh<sub>2</sub>Me ancillary ligands alter the MLCT energy mainly by changing the HOMO energy level. The HOMO energy level of the cis-isomer may be lowered by a high trans effect of the strong-field ancillary ligand, which causes a significant blue shifted emission. It is also likely that the strong-field ancillary ligand PPh<sub>2</sub>Me increases the MLCT characteristics of the cis-isomer by lowering the t<sub>2g</sub> energy level of 5d-orbitals of the metal. We discuss how the ancillary ligand PPh<sub>2</sub>Me influences both the emission peak and the MLCT transition efficiency.*

**Keywords** Blue; cationic iridium complex; LEC; OLED; phosphorescence; TDDFT

## 1. Introduction

Light-emitting electrochemical cells (LECs) have attracted increasing attention in recent years and hold much promise as the next generation of solid-state lighting due to their many advantages over traditional organic light-emitting diodes (OLEDs). LECs are particularly promising for large-area lighting applications because they are easy to produce and operate at very low voltages, yielding highly power-efficient devices. Typical OLEDs require a multilayered structure for charge injection, transport, and light emission, as well as a low work-function metal cathode and a high work-function metal or metal oxide anode to provide efficient charge injection [1–4]. LECs require only a single layer of organic semiconductor, which is processed directly from solution. LECs generally give low turn-on voltages, close to the photon energy, which are largely independent of the thickness of the active

---

Address correspondence to Young Sik Kim, Department of Information Display, Hongik University, Seoul 121-791, Korea. E-mail: youngkim@hongik.ac.kr

layer. Furthermore, charge injection in an LEC is insensitive to the work function of the electrode material, thus permitting the use of a wide variety of metals as cathode materials [5–7].

The first examples of LECs were based on conjugated polymers to which inorganic salts were added [8]. More recently, organometallic compounds that yield single-component solid-state light-emitting devices have attracted wide interest. The majority of the devices is based on charged organometallic complexes using iridium(III) and ruthenium(II) as the metal core [9–11]. The compound most widely used in these single-component devices is tris-(bipyridine) ruthenium(II),  $\text{Ru}(\text{bpy})_3^{2+}$ , balanced by a large negative counter ion such as hexafluorophosphate [12,13]. Thus, LECs based on charged metal complexes do not require the presence of an added electrolyte or an ion-conducting polymer, making the device architecture simpler than that of polymer-based LECs. However, a number of complications remain that impede their integration in products. These include a limited temporal stability and the lack of deep-blue light-emitting complexes. Using various chemical approaches, the range of available colors has recently increased up to a bluish-green device [10].

Mixed ligand cationic iridium complexes of the type  $[\text{Ir}(\text{C}^{\wedge}\text{N})_2(\text{N}^{\wedge}\text{N})]^+$ , with ( $\text{C}^{\wedge}\text{N}$ ) cyclometalating and ( $\text{N}^{\wedge}\text{N}$ ) bipyridine-like ligands, are studied in this respect because the two types of ligands can be almost independently functionalized to obtain the desired color tuning. Electron withdrawing substituents on the phenyl ring of ( $\text{C}^{\wedge}\text{N}$ ) ligands decrease the donation to the metal and therefore stabilize the metal-based HOMO. On the other hand, electron-donating substituents on the ( $\text{N}^{\wedge}\text{N}$ ) ligand lead to destabilization of the ( $\text{N}^{\wedge}\text{N}$ ) ligand-based LUMO, ultimately leading to increased HOMO-LUMO gaps and a blue-green emission at 463 nm with high quantum yield [14,15].

However, purely blue-emitting cationic iridium complexes are rarely found. Recently, cationic iridium(III) complexes with phenylpyridine and phosphines,  $[\text{trans-Ir}(\text{dfMeppy})_2(\text{PPh}_2\text{Me})_2]^+$  and  $[\text{cis-Ir}(\text{dfMeppy})_2(\text{PPh}_2\text{Me})_2]^+$ , [dfMeppy = 2-(2',4'-difluorophenyl)-4-methyl pyridine] were synthesized and studied to tune the phosphorescence wavelength to the deep blue region and to enhance the luminescence efficiencies.  $[\text{Trans-Ir}(\text{dfMeppy})_2(\text{PPh}_2\text{Me})_2]^+$  produce the PL emission at 450 and 475 nm, whereas  $[\text{cis-Ir}(\text{dfMeppy})_2(\text{PPh}_2\text{Me})_2]^+$  emits the PL emission at 442 and 470 nm, respectively [16]. These promising results prompted us to perform a systematic investigation of the photophysical and electrochemical properties of the cationic Ir(III) complexes with different isomeric structures in order to experimentally assess the role of substituents located on various positions of the phosphine ligand.

## 2. Details of the Calculation

To gain insight into the factors responsible for the emission color change and the different quantum yields, we perform density functional theory (DFT) and time-dependent DFT (TDDFT) calculations on the ground and excited states of these complexes, characterizing the excited-state geometries and including solvation effects on the calculation. This computational procedure allows us to provide a detailed assignment of the excited states involved in the absorption and emission processes and to rationalize the factors determining the efficiency of radiative and nonradiative deactivation pathways.

The geometries of all complexes were optimized by DFT method using the B3LYP exchange-correlation function, together with a LANL2DZ (6-31G(d,p))

basis set for Ir (N, C, O, H) in the Gaussian 03 (G03) program package. Electronic populations of the central atom were calculated to show the significant admixture of  $\pi$  character of the ligand and 5d character of the centric Ir metal in HOMOs related to these metal to ligand charge transfer (MLCT) transitions. At the ground-state-optimized geometries, we performed TDDFT calculations at the B3LYP/LANL2DZ level of theory in dichloromethane solution by means of the PCM solvation model, as implemented in the G03 program package. Calculation of the lowest 70 singlet-singlet excitations at the ground-state-optimized geometries allowed us to simulate a large (up to 250 nm) portion of the absorption spectrum. The simulation of the absorption spectra has been performed by a Gaussian convolution with  $\text{fwhm} = 0.4 \text{ eV}$ ; the experimental spectra have been rescaled so that the intensity of the experimental and theoretical main features in the absorption spectra match.

We optimized the geometry of the lowest excited state by means of self-consistent field calculations imposing a triplet spin multiplicity. At the triplet-optimized geometries, we calculated the three lowest singlet-singlet (S) and singlet-triplet (T) TDDFT excitations in dichloromethane at the B3LYP/LANL2DZ level, the triplet excited state being related to the emission process. It should be noted that the singlet-triplet excitation oscillator strengths are set to zero due to the neglect of spin-orbit coupling in the TDDTF calculations as implemented in G03.

### 3. Results and Discussion

To provide detailed insight into the electronic energy levels and nature of the electronic transitions controlling the electrochemical and optical properties, we performed DFT calculations on the cationic iridium complexes. Figure 1 shows  $[\text{trans-Ir}(\text{dfMeppy})_2(\text{PPh}_2\text{Me})_2]^+$  (1) and  $[\text{cis-Ir}(\text{dfMeppy})_2(\text{PPh}_2\text{Me})_2]^+$  (2) containing two dfMeppy ligands trans and cis to each other, respectively. The two nitrogen atoms are cis to each other in trans-isomer 1 but trans to each other in cis-isomer 2. We optimized the singlet ground-state geometries and the lowest triplet excited-state geometries of the cationic complexes. Selected optimized geometrical parameters of

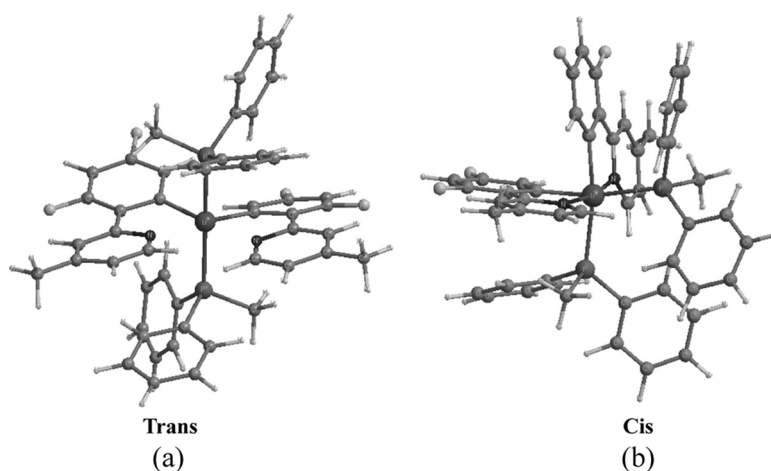


**Figure 1.** Optimized molecular structures of  $[\text{trans-Ir}(\text{dfMeppy})_2(\text{PPh}_2\text{Me})_2]^+$  and  $[\text{cis-Ir}(\text{dfMeppy})_2(\text{PPh}_2\text{Me})_2]^+$ .

the ground compared to the available structural data were obtained from an X-ray investigation of the related complexes [16]. Even though these complexes carry the ppy ligand instead of the dfMeppy ligand, our optimized geometrical parameters are in excellent agreement with the X-ray data. For instance, for the trans-isomer 1, we calculated Ir-N, Ir-C, and Ir-P bond distances and P-Ir-P, C-Ir-N bond angles of 2.238, 2.054, 2.444 Å and 179.1°, 178.8° and compared them to X-ray experimental values of 2.168, 2.052, 2.389 Å and 174.8°, 175°, respectively. For the cis-isomer 2, Ir-N, Ir-C, and Ir-P bond distances and N-Ir-N, C-Ir-P bond angles are calculated at 2.100, 2.053, 2.480 Å and 168.9°, 168.9° and compared to X-ray experimental values of 2.089, 2.072, 2.433 Å and 164.3°, 169.3°, respectively. Interestingly, for trans-isomer 1, we evidenced a significantly lengthened Ir-N bond distance (2.238 vs. 2.100 Å for the trans and the cis-isomer, respectively). This effect is due to the presence of two PPh<sub>2</sub>Me ligands in the trans position, which sterically perturbs the metal coordination sphere, thus producing a strain on the Ir-N bond. A similar effect was found for the X-ray structure due to the presence of bulky PPh<sub>3</sub> in the trans positions [16]. There is a difference in Ir-C bond distance of the cis-isomer (2.072 vs. 2.053 Å for the X-ray data with the ppy ligand and the calculated value with dfMeppy, respectively). This is due to the significant admixture of  $\pi$  character of the dfMeppy ligand and the  $t_{2g}$  energy level of 5d-orbitals of the Ir metal in the cis-isomer. The electron-withdrawing fluoro group in the phenyl ring of dfMeppy decreases the HOMO energy level and the strong-field ancillary ligand PPh<sub>2</sub>Me lowers the  $t_{2g}$  energy level of 5d-orbitals of the Ir metal. It leads to increased mixing between the metal and the dfMeppy ligand and increases the MLCT characteristics. Bond angles show minimal variations among the complexes investigated and are in good agreement with X-ray experimental values.

On the optimized geometries, we performed single-point calculations in dichloromethane solutions. The results, in terms of frontier orbitals, are reported in Figure 2. The solvent was chosen because it experimentally employed for the photophysical measurements. Sizable differences between the trans-isomer and the cis-isomer were found. The HOMO and HOMO-1 of these complexes are a combination of Ir( $t_{2g}$ ) and dfMeppy ( $\pi$ ) orbitals of A symmetry. The HOMO of these complexes are calculated at -6.29, and -6.40 eV for trans-isomer and cis-isomer, respectively. The HOMO of cis-isomer is stabilized compared to that of trans-isomer because of a high trans effect of the strong-field ancillary ligand PPh<sub>2</sub>Me, which causes a significant blue shifted emission. The HOMO-2 of cis-isomer has a same character of HOMO/HOMO-1; however, the HOMO-2 of trans-isomer shows a mixture of  $\pi$  character of PPh<sub>2</sub>Me ligand as a result of the presence of two sterically perturbed PPh<sub>2</sub>Me ligands in the trans position. The LUMO and LUMO + 1 of these complexes are a  $\pi^*$  orbital localized on the dfMeppy ligand acting as an acceptor. However, regarding the trans-isomer, the LUMO + 2 is a  $\pi^*$  orbital localized on the PPh<sub>2</sub>Me ancillary ligand for the same reason as HOMO-2. The electronic populations of Ir orbitals in HOMO are 49.4% cis-isomer and 46.8% trans-isomer. It shows that the strong-field ancillary ligand PPh<sub>2</sub>Me trans to dfMeppy increases the MLCT characteristics of the cis-isomer by lowering the  $t_{2g}$  energy level of 5d-orbitals of the metal to increase the mixing between the metal and the dfMeppy ligand.

The solution UV-Vis absorption of complexes has been calculated as shown in Figure 3. The comparison of calculated values with experimental data is not provided due to the absence of experimental data in Ref. 16. However, inspection of

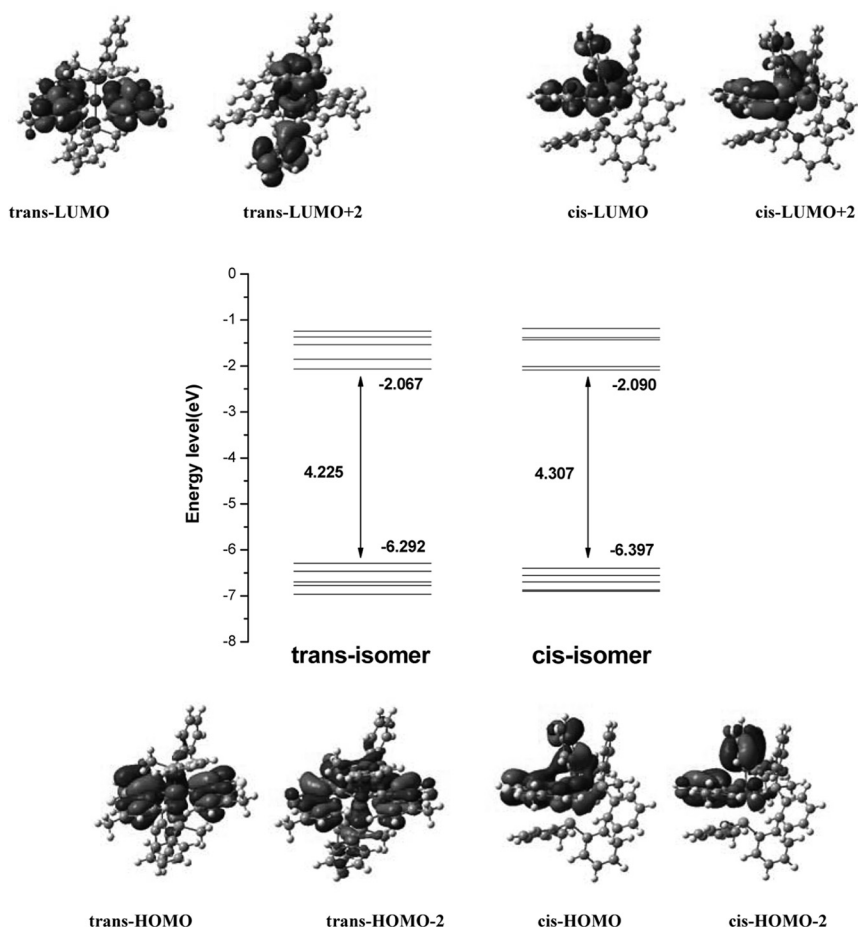


**Figure 2.** Calculated electronic structure in dichloromethane solution for  $[\text{trans-Ir}(\text{dfMeppy})_2(\text{PPh}_2\text{Me})_2]^+$  and  $[\text{cis-Ir}(\text{dfMeppy})_2(\text{PPh}_2\text{Me})_2]^+$  at their optimized geometries of ground electronic state. Also shown are isodensity surface plots of selected molecular orbitals of these complexes.

the TDDFT eigenvectors allows us to assign the three main features giving rise to the 264 nm band as overlapping ligand centered (LC:  $\pi-\pi^*$ ) transitions of the dfMeppy and  $\text{PPh}_2\text{Me}$  ligands, while the transitions giving rise to the 290 nm shoulder appear to be composed by mixed LC and MLCT excitations to the dfMeppy based  $\pi^*$  orbitals for *cis*-isomer, and to the  $\text{PPh}_2\text{Me}$  based  $\pi^*$  orbital for *trans*-isomer. The fact that they are weaker at lower levels of energy ( $>300$  nm) is mainly due to MLCT transitions. At longer wavelengths, we calculate three transitions of sizable intensity at 323, 331, 347 nm ( $f = 0.030, 0.052$  and  $0.040$ ) for *trans*-isomer and at 317, 338 and 345 nm ( $f = 0.017, 0.004$  and  $0.045$ ) for *cis*-isomer, as shown in Figure 3. These three transitions have MLCT character, originating from the HOMO/HOMO-1 set to the LUMO/LUMO + 1 set. For *cis*-isomer, the transitions of 303, 308 and 313 nm have the same MLCT character from the HOMO-1/HOMO-2 set to LUMO/LUMO + 1 set, while the transitions of 301, 304, 308 and 309 nm of *trans*-isomer have the

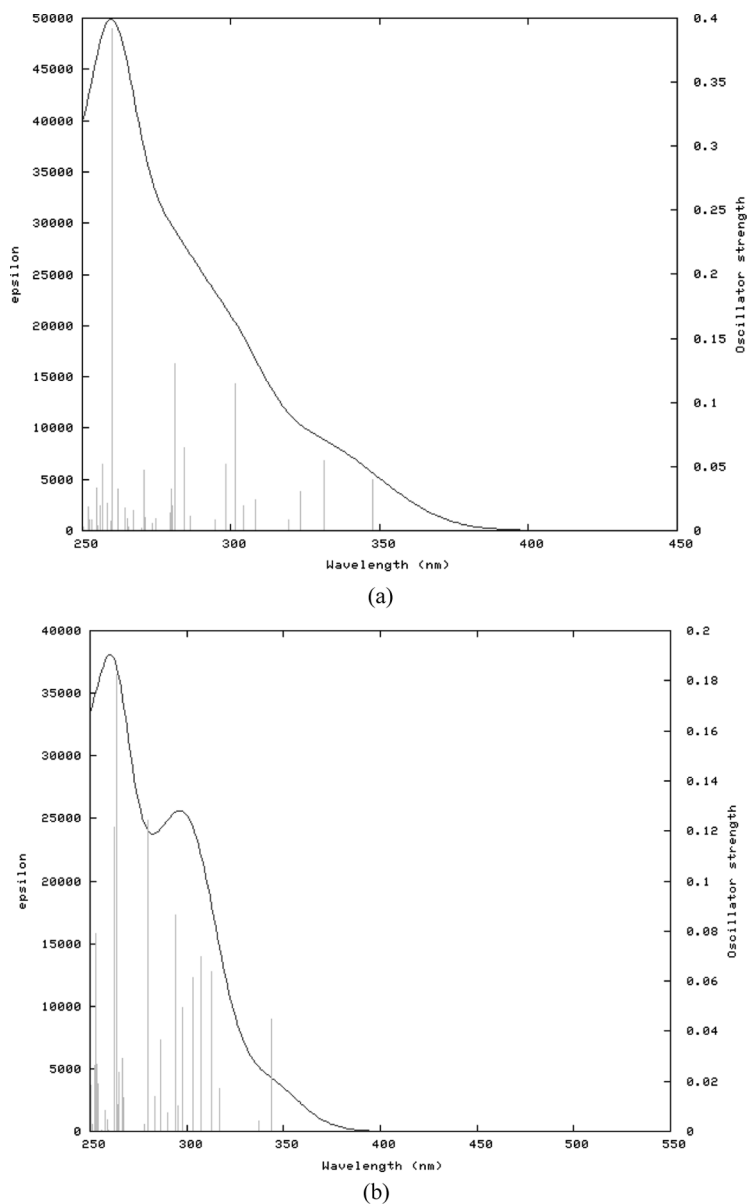


**Figure 3.** Calculated UV-Vis absorption spectrum of (a) [trans-Ir(dfMeppy)<sub>2</sub>(PPh<sub>2</sub>Me)<sub>2</sub>]<sup>+</sup>, and (b) [cis-Ir(dfMeppy)<sub>2</sub>(PPh<sub>2</sub>Me)<sub>2</sub>]<sup>+</sup> in dichloromethane solution.

PPh<sub>2</sub>Me  $\pi^*$  (LUMO + 2) as the arriving state. The intensity difference clearly originates from the different starting and the arriving orbitals.

To gain insight into the nature of the excited states involved in the emission process, we repeated the calculation of the lowest singlet-singlet and singlet-triplet excitation energies at the T<sub>1</sub> optimized geometry. The energies of the lowest excited states calculated in dichloromethane solution for the investigated complexes are reported in Table 1. As it can be seen from Table 1, the emission energies calculated

**Table 1.** Lowest singlet-triplet ( $S_0$ - $T_1$ ) and singlet-singlet ( $S_0$ - $S_1$  and  $S_0$ - $S_2$ ) excitation energies (eV) for trans- and cis-isomers calculated in dichloromethane solution at the  $S_0$  and  $T_1$  optimized geometries. For singlet-singlet excitations, oscillator strengths are also reported. Experimental values [eV (nm)] of the emission maxima for trans- and cis-isomers are reported for comparison

	Trans-isomer		Cis-isomer	
	$S_0$	$T_1$	$S_0$	$T_1$
$S_0$ - $T_1$	2.908	2.542	2.923	2.583
$S_0$ - $S_1$	3.565 (0.040)	3.155	3.584 (0.044)	3.171
$S_1$ - $S_2$	3.742 (0.054)	3.573	3.665 (0.044)	3.592
Emission <sup>a</sup>	2.755 (450)	2.610 (475)	2.805 (442)	2.638 (470)

<sup>a</sup>Emission data were collected from Ref. 16 in eV (nm).

at the  $S_0$  and  $T_1$  optimized geometries nicely correlate with the experimental data of Table 1. In particular, a blue-shift of the lowest excitation energies is calculated on going from trans-isomer to cis-isomer. Comparison of calculated emission energies with emission spectral maxima shows that the PL spectrum of cis-isomer has a significant blue shifted phosphorescence emission due to the strong field ancillary ligand  $PPh_2Me$ , which lowers the  $t_{2g}$  energy level of 5d-orbitals of the Ir metal. It leads to increased mixing between the metal and the dfMeppy ligand and increases the MLCT characteristics. The strong MLCT characteristics of cis-isomer lead to increasing PL efficiency.

#### 4. Conclusions

In summary, we report the theoretical studies of cationic Ir(III) complexes with phenylpyridine and phosphines,  $[trans-Ir(dfMeppy)_2(PPh_2Me)_2]^+$  and  $[cis-Ir(dfMeppy)_2(PPh_2Me)_2]^+$  in order to find a purely blue emitting material for application in LECs. To gain insight into the factors responsible for the emission color change and the different quantum yields, we perform DFT and TDDFT calculations on the ground and excited states of these complexes, including solvation effects on the calculation of the excited states.  $[Trans-Ir(dfMeppy)_2(PPh_3Me)_2]^+$  produces the PL emission at 450 and 475 nm, whereas  $[cis-Ir(dfMeppy)_2(PPh_2Me)_2]^+$  produces the PL emission at 442 and 470 nm, respectively. The computational study allows us to reveal that the position of the  $PPh_2Me$  ancillary ligands alter the MLCT energy mainly by changing the HOMO energy level. The HOMO energy level of the cis-isomer may be lowered by a high trans effect of the strong-field ancillary ligand, which causes a significant blue shifted emission. It is also likely that the strong-field ancillary ligand  $PPh_2Me$  increases the MLCT characteristics of the cis-isomer by lowering the  $t_{2g}$  energy level of 5d-orbitals of the metal. The strong MLCT characteristics of cis-isomer lead to increasing PL efficiency.

#### Acknowledgment

This work was supported by 2010 Hongik University Research Funds.

## References

- [1] Tang, C. W. & VanSlyke, S. A. (1987). *Appl. Phys. Lett.*, *51*, 913.
- [2] Parker, I. D. (1994). *J. Appl. Phys.*, *75*, 1656.
- [3] Hughes, G. & Bryce, M. R. (2005). *J. Mater. Chem.*, *15*, 94.
- [4] (a) Seo, J. H., Kim, I. J., Kim, Y. K., & Kim, Y. S. (2008). *Jpn. J. Appl. Phys.*, *47*, 6987;  
(b) Seo, J. H., Kim, I. J., Kim, Y. K., & Kim, Y. S. (2008). *Thin Solid Films*, *516*, 3614.
- [5] Armstrong, N. R., Wightman, R. M., & Gross, E. M. (2001). *Annu. Rev. Phys. Chem.*, *52*, 391.
- [6] Edman, L., Summers, M. A., Buratto, S. K., & Heeger, A. (2004). *J. Phys. Rev. B*, *70*, 115212.
- [7] Slinker, J., Bernards, D., Houston, P. L., Abruna, H. D., Bernhard, S., & Malliaras, G. G. (2003). *Chem. Commun.*, 2392.
- [8] Pei, Q., Yu, G., Zhang, C., Yang, Y., & Heeger, A. J. (1995). *Science*, *270*, 719.
- [9] Ragni, R., Plummer, E. A., Brunner, K., Hofstraat, J. W., Babudri, F., Farinola, G. M., Naso, F., & De Cola, L. J. (2006). *Mater. Chem.*, *16*, 1161.
- [10] Tamayo, A. B., Garon, S., Sajoto, T., Djurovich, P. I., Tsyba, I., Bau, R., & Thompson, M. E. (2005). *Inorg. Chem.*, *44*, 8723.
- [11] Slinker, J. D., Gorodetsky, A. A., Lowry, M. S., Wang, J., Parker, S., Rohl, R., Bernhard, S., & Malliaras, G. G. (2004). *J. Am. Chem. Soc.*, *126*, 2763.
- [12] Gao, F. G. & Bard, A. J. (2000). *J. Am. Chem. Soc.*, *122*, 7426.
- [13] Handy, E. S., Pal, A. J., & Rubner, M. F. (1999). *J. Am. Chem. Soc.*, *121*, 3525.
- [14] Nazeeruddin, M. K., Weh, R. T., Zhou, Z., Klein, C., Wang, A., De Angelis, F., Fantacci, S., & Gratzel, M. (2006). *Inorg. Chem.*, *45*, 9254.
- [15] De Angelis, F., Fantacci, S., Evans, N., Klein, C., Zakeeruddin, S. M., Moser, J., Kalyanasundaram, K., Bolink, H. J., Gratzel, M., & Nazeeruddin, M. K. (2007). *Inorg. Chem.*, *46*, 5989.
- [16] Chin, C. S., Eum, M., Kim, S. Y., Kim, C., & Kang, S. K. (2006). *Eur. J. Inorg. Chem.*, 4979.